Electronic transport in n- and p-type modulation doped $Ga_xIn_{1-x}N_yAs_{1-y}$/GaAs quantum wells

2009 J. Phys.: Condens. Matter 21 174210

(http://iopscience.iop.org/0953-8984/21/17/174210)

IOP Publishing Journal of Physics: Condensed Matter

J. Phys.: Condens. Matter **21** (2009) 174210 (8pp) doi:10.1088/0953-8984/21/17/174210

Electronic transport in n- and p-type modulation doped $Ga_xIn_{1-x}N_yAs_{1-y}$/GaAs quantum wells

Y Sun[1], N Balkan[1,5], M Aslan[2], S B Lisesivdin[3], H Carrere[4], M C Arikan[2] and X Marie[4]

[1] School of Computer Science and Electronic Engineering, University of Essex, Wivenhoe Park, Colchester CO4 3SQ, UK
[2] Faculty of Science, Department of Physics, Istanbul University, 34134 Istanbul, Turkey
[3] Department of Physics, Faculty of Science and Arts, Gazi University, Teknikokullar, 06500 Ankara, Turkey
[4] Department of Physics, INSA, 135 avenue de Rangeil, 31077 Toulouse cedex 4, France

E-mail: balkan@essex.ac.uk

Received 1 October 2008, in final form 23 November 2008
Published 1 April 2009
Online at stacks.iop.org/JPhysCM/21/174210

Abstract

We present a comprehensive study of longitudinal transport of two-dimensional (2D) carriers in n- and p-type modulation doped $Ga_xIn_{1-x}N_yAs_{1-y}$/GaAs quantum well structures. The Hall mobility and carrier density of electrons in the n-modulation doped quantum wells (QWs) decreases with increasing nitrogen composition. However, the mobility of the 2D holes in p-modulation doped wells is not influenced by nitrogen and it is significantly higher than that of 2D electrons in n-modulation doped material. The observed behaviour is explained in terms of increasing electron effective mass as well as enhanced N-related alloying scattering with increasing nitrogen content.

In order to determine the conduction band (CB) and valence band (VB) structures as well as electron and hole effective masses, the band anticrossing model with an eight-band $\mathbf{k}\cdot\mathbf{p}$ approximation in the Lüttinger–Kohn approach is used. The effects of strain, quantum confinement and the strong coupling between the localized nitrogen states and the CB extended states of GaInAs are considered in the calculations. The results indicate that the nitrogen induces a strong perturbation to the CB of the matrix semiconductor whilst the VB remains unaffected.

The temperature dependent mobility of 2D electron gas is discussed using an analytical model that accounts for the most important scattering mechanisms. The results indicate that the interface roughness and N-related alloy scattering are the dominant mechanisms at low temperatures, while polar optical phonon and N-related alloy scattering limit mobility at high temperatures.

(Some figures in this article are in colour only in the electronic version)

1. Introduction

During the past decade, dilute nitride semiconductor alloys, particularly the quaternary material system of GaInNAs/GaAs, have attracted world-wide attention, because of both the unusual physical properties and potential applications in a variety of optoelectronics devices [1–4]. However, dilute nitrides are yet to be utilized in electronic devices. This is primarily due to the drastic reduction in electron mobility upon the incorporation of nitrogen (typically 200 $cm^2\ V^{-1}\ s^{-1}$ at room temperature in n-type GaInNAs epilayers). Furthermore, the underlying scattering mechanisms responsible for the low electron mobility are yet to be fully understood. Several groups

[5] Author to whom any correspondence should be addressed.

Material	**Thickness** (Å)	**Doping** (cm^{-3})	
GaAs (Cap)	500	Si(Be): $1x10^{18}$	
GaAs (Barrier)	200	Si(Be): $1x10^{18}$	
GaAs (Spacer)	50	UD	
$Ga_{1-x}In_xN_yAs_{1-y}$ QW	70	UD	x 3
GaAs(Spacer)	50	UD	
GaAs(Barrier)	200	Si(Be): $1x10^{18}$	
GaAs (Buffer)	500	UD	
Semi insulating GaAs Substrate			

Figure 1. The layer structure of the samples.

have predicted that alloy scattering induced by nitrogen-related localized states (single N, N–N pairs and higher order clusters) near the band conduction edge is one of the main mechanisms in reducing the electron mobility [5–7]. However, Kurtz *et al* [8] argued that the carrier transport in GaInNAs is limited by large scale material inhomogeneities. Recently, Miyashita *et al* [9] suggested that the electron mobility in n-type GaInNAs films is strongly affected by impurity-like scattering induced by the Si–N complexes. On the other hand, Voltz *et al* [10] reported a much higher electron mobility (2000 $cm^2\ V^{-1}\ s^{-1}$) in Te doped samples. Suzuki *et al* [11] also showed that high electron mobilities could be recovered when the indium concentration is increased, hence the N-related scattering centres are reduced.

In this work, we investigated the electronic properties of 2D carriers in n- and p-type modulation doped $Ga_xIn_{1-x}N_yAs_{1-y}$/GaAs quantum wells with various nitrogen contents. In the conventional modulation doped III–V quantum well structures where the parent donors (Si) are spatially separated from the 2D carriers, electron mobilities are enhanced as a result of the reduced local impurity scattering compared to the doped bulk material. We investigated experimentally the electron and hole mobilities and analysed the results using analytical models taking into account the most relevant scattering mechanisms. The results show clearly striking differences between the transport characteristics of 2D electrons and holes in samples with the same nitrogen composition. These are shown to be fundamentally due to the different effects of nitrogen incorporation on the CB and VB structures.

2. Experiment

The samples investigated in this study are listed in table 1. The samples coded 1930 and 1931 were grown by molecular beam epitaxy (MBE), while samples coded HN004 and HN01 were grown by metal organic vapour phase epitaxy (MOVPE) on semi-insulating GaAs. All the samples are modulation doped (Si for n-type and Be for p-type) with three 7 nm wide GaInNAs quantum wells separated by 20 nm wide doped GaAs barriers. The doped GaAs barriers are separated from the quantum wells by a 5 nm undoped spacer layer as shown in figure 1 to reduce the remote impurity scattering.

In order to establish the presence and the concentrations of nitrogen in the $Ga_{1-x}In_xN_yAs_{1-y}$ quantum wells, continuous

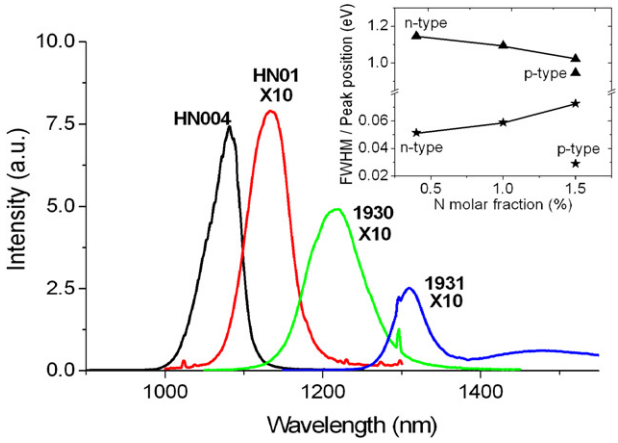

Figure 2. PL spectra of n- and p-type modulation doped $Ga_{1-x}In_xN_yAs_{1-y}$/GaAs MQWs with various nitrogen compositions recorded at 70 K. The inset shows the PL peak position (triangles) and the full width at half maximum (stars) versus nitrogen concentration.

Table 1. Samples used in the investigations.

Sample	Dopant	Indium (%)	Nitrogen (%)	Growth
HN004	Si(n-type)	30	0.4	MOVPE
HN01	Si (n-type)	30	1	MOVPE
1930	Si (n-type)	30	1.5	MBE
1931	Be (p-type)	30	1.5	MBE

wave (CW) photoluminescence (PL) spectra were measured as a function of temperature. The 647 nm line of a Kr-ion laser was used as the excitation source and a 1/3 m, high resolution monochromator in conjunction with a liquid nitrogen cooled InGaAs photomultiplier was employed to disperse and record the PL.

Figure 2 shows the typical PL spectra at 70 K of the four samples investigated. It is clear from figure 2 that increasing the nitrogen concentration red-shifts the emission peak, broadens the spectra line-shape and decreases the PL intensity as commonly reported in dilute nitride semiconductors. The observed shift with increasing nitrogen is in accord with the theoretically calculated transition energies. What is interesting here is that the peak emission energy for the p-modulation doped material is 70 meV below that in the n-modulation

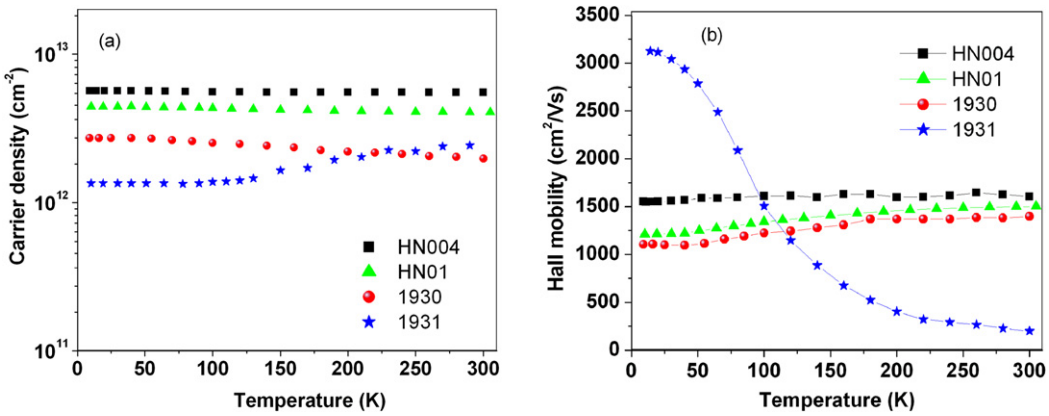

Figure 3. Temperature dependent (a) free carrier density in the quantum well and (b) Hall mobility measured in n- and p-type samples.

doped sample with the same nitrogen content. In the n-type modulation doped material with carrier densities in excess of 10^{12} cm^{-2} (figure 3), all the nitrogen traps are filled; the recombination is via the band-to-band transition involving direct e1–hh1 transitions. However, in the p-type material, the PL emission is due to the recombination of electrons with hh1 holes via the nitrogen-induced defect states. Therefore, the 70 meV difference between the peak energies in the two samples corresponds to the depth of the lowest lying defect states. (A detailed study of the photoluminescence from these samples is given elsewhere [12].)

In order to determine the 2D carrier density and Hall mobility, conventional Hall measurements were carried out in all the samples. Samples were fabricated in the form of Hall bars with channel lengths of 1.75 mm and widths of 0.2 mm. Ohmic contacts were formed by alloying Au/Au:Ge/Ni and Au/Au:Zn for n-type and p-type material respectively. Hall measurements were recorded at lattice temperatures between 9 and 300 K, and at low enough applied electric fields to avoid Joule heating. As a result, both the Hall mobility and carrier density were independent of applied electric field.

Figures 3(a) and (b) show the temperature dependence of the carrier densities and mobilities in all four samples studied. It is clear from figure 3(a) that the free electron density in the n-type samples decreases with the increasing nitrogen concentration, as supported by the reduced intensity of the PL (figure 1), indicating enhanced N-induced trap density in GaInNAs channels.

The Hall data in figures 3(a) and (b) show the clear difference between the temperature behaviour of n- and p-type samples. In the p-doped sample, the hole mobility ($u_{\mathrm{H}} \approx 3125$ cm^2 V^{-1} s^{-1}) is much higher than the electron mobility in n-doped samples at low temperatures. In fact, it is almost a factor of three higher than the corresponding electron mobility ($u_{\mathrm{H}} \approx 1100$ cm^2 V^{-1} s^{-1}) in the sample with the same nitrogen content. Furthermore, the hole mobility exhibits the characteristic temperature dependence of the 2D carriers as observed in N-free GaInAs heterostructures. It has a very weak temperature dependence below $T = 30$ K then decreases rapidly with increasing temperature, as expected for the enhanced polar optical phonon scattering. The electron mobility is not only considerably lower than that in the GaInAs heterostructures but also strongly reduced with increasing N concentration. This is expected as a result of strong resonant scattering induced by N-related localized states [13]. In addition, the electron mobility shows rather weak temperature dependence. This weak temperature dependence of electron mobility was also observed by several groups who reported a strong ionized impurity scattering temperature dependence ($T^{3/2}$) at low temperatures. This behaviour is explained in terms of both the N-related compositional fluctuation with highly localized states close to the CB edge, and non-substitutional N defects such as N–N split interstitials and N–As split interstitials [14–17], which may trap the carriers and act as ionized impurity scattering centres, leading to further reduction in electron mobility. However, this effect is not obvious in our results, where the mobility remains almost constant at low temperatures. The reason for this is probably associated with the screening by high carrier densities in the QWs resulting in the observed enhanced mobility and the lack of strong temperature dependence. These observations are also in accord with the lack of the S-shape temperature dependent behaviour of PL intensity in these samples as reported by us [12]. We show in the following sections that electron mobility in GaInNAs QWs is mainly determined by the N-induced alloy and interface roughness scattering at low temperatures, and limited by polar optical phonon and alloy scattering at high temperatures.

It should be noted that the temperature behaviour of the Hall density and mobility may be analysed in terms of two parallel conducting channels, i.e. quantum wells and the barriers where the relative densities and mobilities change with temperature.

In the n-type material, following the analysis given by Kane *et al* [18], we can write the expressions for the effective Hall mobility and carrier density of the two n-type conducting channels as

$$n_{\mathrm{H}} = \frac{(n_1\mu_1 + n_2\mu_2)^2}{n_1\mu_1^2 + n_2\mu_2^2}$$
$$\mu_{\mathrm{H}} = \frac{n_1\mu_1^2 + n_2\mu_2^2}{n_1\mu_1 + n_2\mu_2} \qquad (1)$$

where n_1/μ_1 and n_2/μ_2 are the electron densities/mobilities in the GaInNAs QWs and Si doped GaAs barriers and n_2, μ_1,

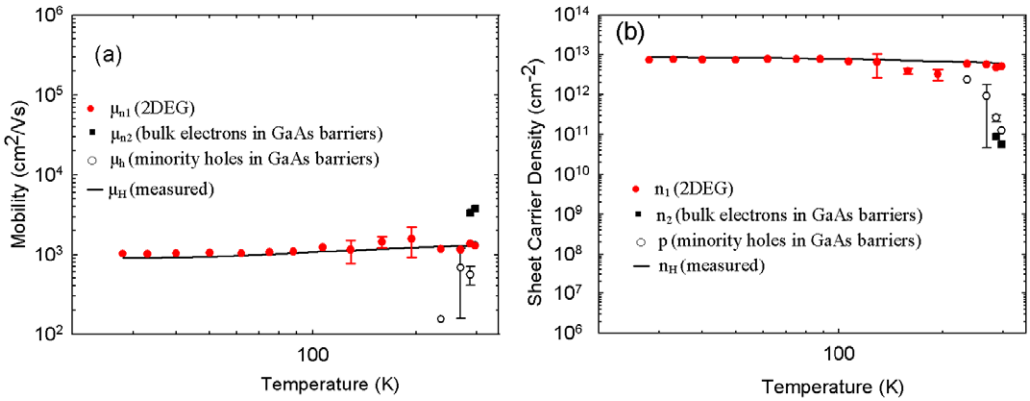

Figure 4. Temperature dependence of (a) mobility and (b) density of sheet carriers in the quantum wells and in the barriers as obtained from QMSA for sample 1930. The temperature dependent Hall mobility and sheet carrier density measured at $B = 0.5$ T are also shown (solid line).

and μ_2 are all temperature dependent. At low temperatures conductivity is due to conduction in the quantum wells because of the carrier freeze-out in the doped GaAs barriers ($n_1 \gg n_2$). Therefore, the Hall mobility and carrier density at low temperatures correspond to conduction in the quantum wells, i.e. $\mu_H(0) = \mu_1$ and $n_H(0) = n_1$. At room temperature the measured Hall carrier density in the n-type material is smaller than the low temperature carrier density, and the measured mobility is considerably higher than the low temperature mobility. This observation can be explained if

$$\begin{aligned} \mu_2(T) > \mu_1(T) \qquad & \text{when } T \to 300 \text{ K} \\ n_2(T) \leqslant n_1(T). & \end{aligned} \tag{2}$$

Therefore, the Hall carrier density and mobility will be a complicated function of temperature as determined by the temperature dependence of the scattering mechanisms in the quantum wells and the GaAs barriers.

In order to extract the temperature dependent mobility of the 2D electron gas in the quantum wells, we carried out the Hall measurements as a function of magnetic field over a temperature range of 28–300 K. The magnetic field dependent Hall data were then analysed using the quantitative mobility spectrum analysis (QMSA) technique, which allows individual carrier density and mobility to be extracted from mixed conduction due to either types of carrier in multilayered semiconductors. This technique has been successfully used by us to investigate the transport properties in AlGaN/GaN heterostructures [19, 20]. Figures 4(a) and (b) show the extracted mobility and integrated carrier density as a function of temperature using the QMSA technique for sample 1930. The Hall mobility and carrier density measured at $B = 0.5$ T are also shown in figure 4.

The QMSA analysis indicates clearly that electron density in the GaAs barriers is around $n_2 \sim 8 \times 10^{10} \pm 50\%$ cm^{-2}, and due to their high mobility ($\mu_2 \sim 3000$ cm^2 V^{-1} s^{-1}) they contribute to the overall conductivity at high temperatures of around 300 K. In addition to electrons, the thermal equilibrium holes in the GaAs barriers are observed to contribute to the overall conductivity at high temperatures, inducing some degree of further parallel conduction. However, the carrier densities of both electrons and holes in the GaAs barriers are much lower than that of 2DEG ($n \sim 7.6 \times 10^{12}$ cm^{-2}) in the wells. Therefore, the effect of parallel conduction induced by minority carriers is negligible and the overall conductivity is thus dominated by the 2DEG in the modulation doped quantum wells and our interpretation of the Hall data in terms of transport of the 2D carriers is plausible.

3. Analysis and discussion of results

3.1. Transport properties of 2D hole and electron gases

In order to determine whether the observed difference in the electron and hole mobilities is intrinsic and associated with the disparity in their effective masses, we carried out a detailed modelling of the $Ga_xIn_{1-x}N_yAs_{1-y}$ conduction and VB structures and obtained the electron and hole effective masses. The band structure of $Ga_xIn_{1-x}N_yAs_{1-y}$/GaAs QWs is calculated by solving the modified eight-band $\mathbf{k}\cdot\mathbf{p}$ Lüttinger–Kohn Hamiltonian, including tetragonal strain and strong coupling between the GaInAs CB and the localized nitrogen levels. The eigenvalue problem is then solved by the transfer matrix method, taking into account the interfacial discontinuity condition [21, 22]. The valence band (VB) material parameters used for the calculations are the ones of GaInAs [23]. As far as the CB is concerned, the energy level of nitrogen (E_N) is assumed to be constant relative to the vacuum level whatever the In concentration is. The In fraction dependence of E_N just reflects the variation of the valence band offset with respect to GaAs [24]. Moreover, the coupling parameter in the band anticrossing model (BAC), V_{NM}, that is given as a function of only N concentration, has been taken as dependent on both In and N compositions. Because the aim of this work is to investigate the transport properties of 2D carriers, therefore, the details of the theoretical model used in this work are not given here and only calculated effective masses of carriers lying band-edge for e1 and hh1 levels in the GaInNAs quantum well are tabulated in table 2. The calculation indicates that the presence of nitrogen induces strong perturbation mainly

Table 2. Theoretically calculated values of the band-edge effective mass for the e1 level and hh1 level in the GaInNAs quantum well.

Sample	Nitrogen (%)	Electron effective mass (m^*_{e1})	Heavy hole effective mass (m^*_{hh1})
HN004 (n-doped)	0.4	$0.069m_0$	$0.11m_0$
HN01(n-doped)	1	$0.076m_0$	$0.105m_0$
1930 (n-doped)	1.5	$0.08m_0$	$0.105m_0$
1931(p-doped)	1.5	$0.08m_0$	$0.105m_0$
N-free GaInAs	0	$0.054m_0$	$0.105m_0$

on the conduction states by mutual repulsion between the CB edge state and localized N states, leading to enhanced non-parabolicity of CB in GaInNAs. Therefore, the electron effective mass increases with increasing nitrogen content even at the CB edge. However, the nitrogen incorporation has negligible effect on the valence band (VB), thus the hole effective mass is independent of nitrogen composition. As a result, the effective masses and mobilities for electrons and holes at elevated nitrogen concentration (1.5% for n-doped sample 1930 and p-doped sample 1931) should be similar. However at low temperatures the hole mobility is a factor of 3 higher than the corresponding electron mobility. We believe, therefore, that the higher hole mobility may be attributed to the lack of scattering from the nitrogen complex whilst the effective mass remains unchanged compared to that in GaInAs. The electron mobility decreases as N concentration increases, which can be explained by both the increasing effective mass and the enhanced N-related alloy scattering. In addition, the nitrogen induces the flattening of the lower sub-band, giving rise to an enhanced density of states of electrons at the CB edge. Therefore, the density of electrons is expected to be higher than that of holes in the GaInNAs QWs with the same nitrogen concentration, as observed in figure 3(a) at low temperatures.

In the p-modulation doped sample at high temperatures (above 150 K), the Hall density represents a combination of the 2D hole gas in the quantum wells and the holes in the wide GaAs barriers due to the full ionization of acceptors further away from the depletion regions as well as the thermionic emission of holes from the quantum wells over the shallow barriers, $V_B = 110$ meV [25].

3.2. 2DEG mobility analysis

In order to evaluate the temperature dependence of the electron mobility, different scattering mechanisms have been considered. The final carrier mobility μ_{tot} was then obtained using Matthiessen's rule:

$$\mu_{tot} = \left(\sum_i \frac{1}{\mu_i}\right)^{-1} \tag{3}$$

where μ_i is the mobility due to the ith scattering mechanism. For simplicity, we assume that electrons are confined to the lowest sub-band in an infinite square quantum well and the interaction with phonons is confined to the same quantum well. In addition, the isolated nitrogen state lies about 480 meV at RT and 410 meV at 10 K above the band-edge of the lowest sub-band in the quantum well calculated for sample 1930. We assume all carriers lying at the bottom of the CB minimum (CBM) at low electric fields; therefore, it is acceptable to calculate electron mobility using parabolic energy dispersion. The analytical expressions of the scattering mechanisms used in the calculation are summarized below. The material parameters used in the calculations for sample 1930 ($y = 0.015$) are also listed in table 3.

Table 3. Values of material constants used in the calculation for sample 1930 [45–47].

Electron effective mass	$m^*_{e1} = 0.08m_0$
High frequency dielectric constant	$\varepsilon_\infty = 11.11$
Static dielectric constant	$\varepsilon_s = 13.575$
LO phonon energy	$\hbar\omega = 36$ meV
Quantum well width	$L = 7$ nm
Lattice constant of GaInAs	$a_0 = 5.7668$
Energy of isolated nitrogen	$E_N = 1.67$ eV
Interaction strength of the isolated nitrogen	$\beta = 1.675$ eV
Electron wavevector	$k = 4.1416 \times 10^8$ m^{-1}
Carrier density of 2DEG	$n_{2D} = 2.73 \times 10^{16}$ m^{-2}

3.2.1. Polar optical phonon scattering. In usual N-free heterostructures, the mobility is limited by optical phonon scattering at high temperatures. Therefore, the optical phonon is also considered in the diluted nitride system. The expression of the mobility limited by polar optical phonon scattering is given by Ridley [26]

$$\mu_{po} = \frac{4\pi\varepsilon_0\varepsilon_p\hbar^3}{e\hbar\omega m^{*2}L}\left[e^{\hbar\omega/k_BT} - 1\right] \qquad \text{where } \frac{1}{\varepsilon_p} = \frac{1}{\varepsilon_\infty} - \frac{1}{\varepsilon_s}. \tag{4}$$

Here, $\hbar\omega$ is the polar optic phonon energy; ε_∞ and ε_s are the high and low frequency dielectric constants, respectively; m^* and L are the electron effective mass and width of the quantum well, respectively.

3.2.2. Alloy scattering. The electron mobility in dilute nitride is intrinsically limited by strong N-related alloy scattering. Recently, the relaxation rate of resonant scattering due to the substitutional N for 2DEG electron was derived by Fahy *et al* using the linear combination of isolated nitrogen states (LCINS) approach incorporating hybridization with a full range of nitrogen-related cluster states, and can be expressed as [7]

$$R_{all,QW}(E) = \frac{3\pi a_0^3 m^*}{8L\pi\hbar^3}\frac{1}{N_a}\sum_i \frac{\beta'^4}{(E - E_i)^2 + (\Gamma_{av,i}/2)^2} \tag{5}$$

where N_a, a_0 and $\hbar$ are the number of primitive cells, lattice constant of GaInAs and reduced Planck's constant, respectively; $E_i, \Gamma_{av,i}$ and $\beta'_i = \beta\sqrt{f_T}$ are energies, energy broadenings and effective interaction strength of the ith nitrogen cluster, respectively. The carrier mobility can then be

obtained from the Boltzmann transport equation and is given by [7]

$$\mu_{\rm all} = \frac{j_{\rm QW}}{en_{\rm 2D}F} = \frac{{\rm e}^2F}{en_{\rm 2D}F(2\pi\hbar)^2}\int_0^\infty \frac{p^2}{m^{*2}R_{\rm all,QW}(E)} \times \frac{\partial f_0}{\partial E}2\pi p\,{\rm d}p \tag{6}$$

where $j_{\rm QW}$, $n_{\rm 2D}$, F, f_0 and p are current density, carrier density, electric field, Fermi–Dirac distribution and momentum at energy E, respectively. By substituting equation (5) into equation (6), we have

$$\mu_{\rm all} = \frac{16eL\hbar^3}{3m^{*2}(a_0)^3}\frac{1}{\ln(1+{\rm e}^\eta)}\int_0^\infty \frac{{\rm e}^{u^2-\eta}u^3\,{\rm d}u}{M_{\rm QW}(kTu^2)[{\rm e}^{u^2-\eta}+1]^2} \tag{7}$$

where $\eta = (E_{\rm F} - E_{\rm C,QW})/kT$; $E_{\rm C,QW}$ is the CB edge of the lowest sub-band in the QW and the Fermi level, $E_{\rm F}$, can be obtained from the measured sheet carrier density by

$$n_{\rm 2D} = \frac{m^*kT}{\pi\hbar^2}\ln\left[1+{\rm e}^{\frac{E_{\rm F}-E_{\rm C,QW}}{kT}}\right]. \tag{8}$$

At $T = 0$ K, equation (6) reduces to the familiar expression

$$n_{\rm 2D} = \frac{m^*}{\pi\hbar^2}(E_{\rm F} - E_{\rm C,QW}) \tag{9}$$

and

$$M_{\rm QW}(u) = \frac{1}{N_a}\sum_i \frac{\beta'^4}{(E_{\rm C,QW}+kTu^2-E_i)^2+(\Gamma_{{\rm av},i}/2)^2}. \tag{10}$$

In the GaNAs material, the effect of N–N pairs and higher order clusters on the electron mobility has to be considered due to nitrogen pairs and larger cluster states near the CB edge [5, 7]. In the case of GaInNAs, the replacement of gallium by indium shifts the host CB edge downward, and also pushes the energy of the N cluster states upward relative to the cluster state energies in GaNAs [27]. The N–N energy relative to the GaAs valence band maximum (VBM) is about 1.51 eV, which gives about 260 meV (RT) and 190 meV (10 K) above the CB edge of GaInNAs calculated for sample 1930 using model solid theory taking the equation (strain effect into account [28, 29]. In addition, we assume the nitrogen distribution is random, then the concentration of N–N pairs is much smaller than that of isolated nitrogen (12% of N atoms in N–N pairs) [5]; therefore, it is reasonable to calculate the alloy scattering rate by neglecting the effect of N–N pairs. The scattering rate is further simplified by making the assumption that all clusters of same type have the same energy and interaction strength; and the interaction between nitrogen-induced localized states is neglected. The scattering rate is then reduced to the BAC model (only two bands considered and the energy broadening is neglected) and is similar to the calculation deduced by Vaughan *et al* [30] using the n-band model. Equation (10) then can be simplified and reduced to

$$M_{\rm QW}(u) = \frac{\beta^4 y}{(E_{\rm C,QW}+kTu^2-E_{\rm N})^2+(\Gamma_{\rm av}/2)^2} \tag{11}$$

where y and $E_{\rm N}$ are the concentration and energy of isolated nitrogen, respectively. $E_{\rm C,QW}$ is calculated using the BAC model taking the strain effect into account and is shifted by infinite quantum well confinement (${\rm d}E = \frac{\hbar^2\pi^2}{2m^*L^2}$). All energies are aligned to the VB edge of GaAs. Here the energy broadening is given by

$$\Gamma_{\rm av} = 2\pi\sqrt{\frac{3}{2}}\beta^2\frac{(a_0)^3m^*}{8L\pi\hbar^2}. \tag{12}$$

In order to confirm the current model, the mobility limited by alloy scattering for sample 1930 was calculated taking the parameters given in table 3. The results were compared to the carrier mobility in GaNAs QW calculated by Vaughan *et al* [31] using non-parabolic band structure as shown in figure 3. The temperature dependence of the mobility is in good agreement with that modelled by Vaughan *et al* for the 10 nm GaNAs quantum wells, which is of comparable width to the QWs in our samples.

In contrast to the mobility in the bulk dilute nitride, where the mobility strongly depends upon temperatures as $\propto T^{-1/2}$; the 2DEG mobility exhibits much weaker temperature dependence, and increases slightly with increasing temperature [6]. As the quantum well becomes wider, the 2DEG mobility is more bulk-like and shows strong temperature dependence, as shown in figure 5(b). In GaInNAs material, the electron mobility should be higher than that in GaNAs due to the effect of indium, which reduces the interaction strength between N and the CB edge and also pushes the CB edge $E_{\rm C,QW}$ far below the energy level of nitrogen complexes [32–35].

3.2.3. Interface roughness scattering. In dilute nitrides the almost inevitable presence of alloy fluctuations, impurities and interface imperfections leads to the perturbation of the electron confinement energy [36, 37]. The PL spectra of different samples cleaved from the same wafer shift by about 15 nm, corresponding to about 1–2 monolayer (ML) fluctuations in the well width, strongly suggesting the presence of interface roughness, which can become one of the dominant mechanisms at low temperatures. The interface roughness (IFR) in QWs is usually described by the lateral size Λ and height Δ of the Gaussian fluctuation of the interface and can be expressed as [38, 39]

$$\langle\Delta(\vec{r})\Delta(\vec{r}')\rangle = \Delta^2\exp\left(-\frac{|\vec{r}-\vec{r}'|^2}{\Lambda^2}\right) \tag{13}$$

where $\vec{r}$ and $\vec{r}'$ are the 2D spatial coordinates. The mobility due to the interface roughness including 2D screening is then obtained as [40, 41]

$$\mu_{\rm IFR} = \frac{e\pi\hbar^3}{m^{*2}}\frac{1}{\int_0^{2k}\frac{|M_q|^2}{2k^3(q+q_{\rm s})^2}\frac{q^4{\rm d}q}{\left(1-\left(\frac{q}{2k}\right)^2\right)^{1/2}}} \tag{14}$$

where k is the wavevector, q is the wavevector transferred in a scattering event, M_q is a scattering matrix element and can be

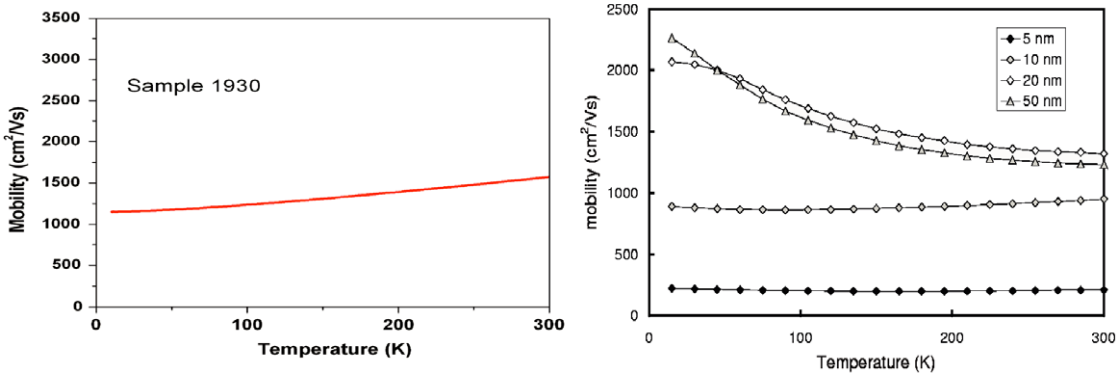

(a) (b)

Figure 5. Calculated mobility limited by alloy scattering versus temperature: (a) current model; (b) calculated by Vaughan *et al* for varying GaNAs quantum well widths (5, 10, 20, and 50 nm) using a non-parabolic band structure [28].

calculated for the case of infinite quantum well [39]

$$M_q^2 = \frac{\pi^5 \hbar^4 \Delta^2 \Lambda^2}{m^{*2} L^6} \exp\left(\frac{-\Lambda^2 q^2}{4}\right) \tag{15}$$

and q_s is the two-dimensional reciprocal screening length and is defined as (in the static limit) [42]

$$q_s = \frac{e^2 m^*}{2\pi\hbar^2 \varepsilon_0 \varepsilon_s} F_{11}(q) f(0) \tag{16}$$

where $f(0)$ is the occupation probability at the lowest sub-band-edge and $F_{11}(q)$ is the form factor and is given by

$$F_{11}(q) = \frac{2}{qL} + \frac{qL}{(qL)^2 + 4\pi^2} - \frac{32\pi^4}{(qL)^2[(qL)^2 + 4\pi^2]^2}(1 - e^{-qL}). \tag{17}$$

In the case of $k_B T \ll E_F$, the mobility can be simplified as $\mu = \frac{e\tau(E_F)}{m_e^*}$, thus the electron wavevector k can be calculated using $k = \sqrt{2\pi n_{2D}}$ [43].

3.2.4. Other scattering mechanisms. In the usual N-free polar materials, scattering mechanisms such as deformation potential, acoustic phonons and piezoelectric acoustic phonon scattering, which limit the electron mobility at intermediate temperatures, need to be considered for mobility analysis. However, in GaInNAs material, the relaxation time of N-induced alloy scattering is almost three orders of magnitude smaller than that of acoustic phonon scattering at room temperature [44]. Therefore, the electron mobility, limited by acoustic phonons, is negligible and is not considered for 2D mobility analysis.

The mobilities limited by individual scattering mechanisms have been calculated for sample 1930 taking the material constants given in table 3. The total mobility was then calculated using Matthiessen's rule. In order to calculate the mobility due to the interface roughness, the height Δ was taken as 2×2.83 (corresponding to two monolayers) and the lateral size Λ was used as an adjustable parameter. In figure 6 we show the calculated individual mobilities and total mobility as a function of temperature for sample 1930. The experimental 2DEG mobility extracted by QMSA is also shown in figure 6 to compare the results. It is clear from figure 6 that the total mobility fits quite well to the experimental data taking the value of lateral size as $\Lambda = 23.4$ Å. The results indicate that the low temperature mobility is dominated by both the interface roughness scattering and N-induced alloy scattering. However, at high temperatures, alloy scattering and polar optical phonon scattering are the dominant mechanisms, and interface roughness scattering only has a small contribution to the mobility of the 2DEG.

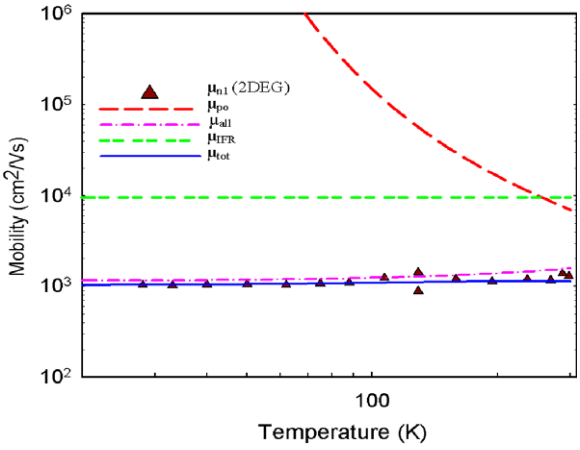

Figure 6. Calculated mobility verses absolute temperature compared to extracted 2DEG mobility using the QMSA technique for sample 1930. Here μ_{po} refers to optical phonon scattering, μ_{all} refers to alloy scattering, μ_{IFR} refers to interface roughness scattering and μ_{tot} refers to calculated total mobility.

4. Summary

In conclusion, we have investigated electronic transport properties of n- and p-type modulation doped GaInNAs/GaAs quantum well structures with various nitrogen compositions. The discrepancy between electron mobility and hole mobility has been observed and discussed in terms of the different

responses of the conduction and valance band structures and hence the effective mass to varying nitrogen concentration as well as the strong alloying scattering that limits the former. The temperature dependence of electron mobility is discussed by using an analytical model taking into account the most relevant scattering mechanisms. The results indicate that the 2DEG mobility in GaInNAs is higher than those reported in GaNAs due to the presence of In atoms, and exhibits a much weaker temperature dependence, probably associated with the screening effect induced by high carrier density in our samples. Finally, we show that the 2DEG mobility is fundamentally limited by the scattering from N complexes.

Acknowledgments

We would like to thank LAAS-CNRS in Toulouse (FR) and the University of Helsinki for supplying the samples. Part of this work was carried out at Istanbul University and was supported by the Research Fund of Istanbul University (project number BYP 2237) and TR Prime Ministry State Planning Organization (project number 2005K-120430).

References

[1] As review see, special issues, Dilute Nitrides 2004 *J. Phys.: Condens. Matter* **16** 31
[2] Tournie E, Pinault M-A, Laugt M, Chauveau J-M, Trampert A and Ploog K H 2003 *Appl. Phys. Lett.* **82** 1845
[3] Harris J S 2002 *Semicond. Sci. Technol.* **17** 880
[4] Yamaguchi M 2002 *Physica* E **14** 84
[5] Fahy S, Lindsay A and O'Reilly E P 2004 *IEE Proc. Optoelectron.* **151** 352
[6] Fahy S and O'Reilly E P 2003 *Appl. Phys. Lett.* **83** 3731
[7] Fahy S, Lindsay A, Ouerdane H and O'Reilly E P 2006 *Phys. Rev.* B **74** 035203
[8] Kurtz S R, Allerman A A, Seager C H, Sieg R M and Jones E D 2000 *Appl. Phys. Lett.* **77** 400
[9] Miyashita N, Shimizu Y and Okada Y 2007 *J. Appl. Phys.* **102** 044904
[10] Voltz K, Koch J, Kunert B and Stolz W 2003 *J. Cryst. Growth* **248** 451
[11] Suzuki T, Yamaguchi T, Yamamoto A and Hashimoto A 2003 *Phys. Status Solidi* c **0** 2769
[12] Sun Y, Erol A, Yilmaz M, Arikan M C, Ulug B, Ulug A, Balkan N, Sopanen M, Reentilä O, Mattila M, Fontaine C and Arnoult A 2008 *Opt. Quantum Electron* **44** 467–4
[13] Matsuoka T, Kobayashi E, Taniguchi K, Hamaguchi C and Sasa S 1990 *Japan. J. Appl. Phys.* **29** 2017
[14] Mouillet R, de Vaulchier L A, Deleporte E, Guldner Y, Travers L and Harmand J C 2003 *Solid State Commun.* **126** 333
[15] Fowler D, Makarovsky O, Patanè A and Eaves L 2004 *Phys. Rev.* B **69** 153305
[16] Zhang S B and Wei S H 2001 *Phys. Rev. Lett.* **86** 1789
[17] Zhang S B, Janotti A, Wei S-H and de Walle C G V 2004 *IEE Proc. Optoelectron.* **151** 369
[18] Kane M J, Apsley N, Anderson D A, Taylor L L and Kerr T 1985 *J. Phys. C: Solid State Phys.* **18** 5629
[19] Lisesivdin S B, Acar S, Kasap M, Ozcelik S, Gokden S and Ozbay E 2007 *Semicond. Sci. Technol.* **22** 543
[20] Lisesivdin S B, Demirezen S, Caliskan M D, Yildiz A, Kasap M, Ozcelik S and Ozbay E 2008 *Semicond. Sci. Technol.* **23** 095008
[21] Epenga R, Schuurmans M F H and Colak S 1987 *Phys. Rev.* B **36** 1554
[22] Ahn D and Chuang S L 1990 *IEEE J. Quantum Electron.* **26** 13
[23] Vurgaftman I, Meyer J R and Ram-Mohan L R 2001 *Appl. Phys. Lett.* **89** 5815
[24] Marie X, Barrau J, Amand T, Carrère H, Arnoult A, Fontaine C and Bedel-Pereira E 2003 *IEE Proc. Optoelectron.* **150** 25
[25] Sun Y, Balkan N, Erol A and Arikan M C 2009 at press
[26] Ridley B K 1982 *J. Phys. C: Solid State Phys.* **15** 5899
[27] O'Reilly E P, Lindsay A and Fahy S 2004 *J. Phys.: Condens. Matter* **16** S3257
[28] Liu X, Pistol M-E, Samuelson L, Schwetlick S and Seifert W 1990 *Appl. Phys. Lett.* **56** 1451
[29] Van de Walle C G and Martin R M 1987 *Phys. Rev.* B **35** 8154
[30] Vaughan M P and Ridley B K 2007 *Phys. Rev.* B **75** 195205
[31] Vaughan M P 2008 at press
[32] Choulis S A, Tomic S, O'Reilly E P and Hosea T J C 2003 *Solid State Commun.* **125** 155
[33] Choulis S A, Hosea T J C, Tomic S, Kamal-Saadi M, Adams A R, O'Reilly E P, Weinstein B A and Klar P J 2002 *Phys. Rev.* B **66** 165321
[34] Polimeni A, Capizzi M, Geddo M, Fischer M, Reinhardt M and Forchel A 2001 *Phys. Rev.* B **63** 195320
[35] Vurgaftman I and Meyer J R 2003 *J. Appl. Phys.* **94** 3675
[36] Warwick C A, Jan W J and Ourmazd A 1990 *Appl. Phys. Lett.* **56** 2666
[37] Tanaka M and Sakaki H 1987 *J. Cryst. Growth* **81** 513
[38] Balkan N, Gupta R, Cankurtaran M, Çelik H, Bayrakli A, Tiras E and Arikan M Ç 1997 *Superlatt. Microstruct.* **22** 263
[39] Sakaki H, Noda T, Hirakawa K, Tanaka M and Matsusue T 1987 *Appl. Phys. Lett.* **51** 1934
[40] Gold A 1987 *Phys. Rev.* B **35** 723
[41] Gold A and Dolgopolov V T 1986 *Phys. Rev.* B **33** 1076
[42] Ando T, Fowler A B and Stern F 1982 *Rev. Mod. Phys.* **54** 437
[43] Laikhtman B and Kiehl R A 1993 *Phys. Rev.* B **47** 10515
[44] Vaughan M P 2007 *PhD Thesis* University of Essex unpublished
[45] Choulis S A, Tomic S, O'Reilly E P and Hosea T J C 2003 *Solid State Commun.* **125** 155
[46] Choulis S A, Hosea T J C, Tomic S, Kamal-Saadi M, Adams A R, O'Reilly E P, Weinstein B A and Klar P J 2002 *Phys. Rev.* B **66** 165321
[47] Polimeni A, Capizzi M, Geddo M, Fischer M, Reinhardt M and Forchel A 2001 *Phys. Rev.* B **63** 195320